arXiv:1610.03590v1 [cond-mat.mes-hall] 12 Oct 2016

Quantized magnetization density in periodically driven systems

Frederik Nathan[1], Mark S. Rudner[1], Netanel H. Lindner[2], Erez Berg[3] and Gil Refael[4]
[1] *Niels Bohr Institute, University of Copenhagen, 2100 Copenhagen, Denmark*
[2] *Physics Department, Technion, 320003 Haifa, Israel*
[3] *Department of Condensed Matter Physics, The Weizmann Institute of Science, Rehovot, 76100, Israel*
[4] *Institute for Quantum Information and Matter, Caltech, Pasadena, California 91125, USA*
(Dated: October 13, 2016)

We study micromotion in two-dimensional periodically driven systems in which all bulk Floquet eigenstates are localized by disorder. We show that this micromotion gives rise to a quantized time-averaged magnetization density when the system is filled with fermions. Furthermore we find that a quantized current flows around the boundary of any filled region of finite extent. The quantization has a topological origin: we relate the time-averaged magnetization density to the winding number characterizing the new phase identified in Phys. Rev. X **6**, 021013 (2016). We thus establish that the winding number invariant can be accessed directly in bulk measurements, and propose an experimental protocol to do so using interferometry in cold atom based realizations.

Time-periodic driving was recently introduced as a means for achieving topological phenomena in a wide variety of quantum systems. In addition to providing new routes to obtaining topologically nontrivial band structures [1–15], periodic driving can give rise to wholly new types of topological phenomena without analogues in equilibrium [16–28]. The extent to which topological periodically-driven systems behave analogously to their non-driven counterparts, and the range of new types of phenomena that may be discovered, remain very active and interesting subjects of investigation.

In a periodically driven system, the unitary Floquet operator acts as a generator of discrete time evolution over each full driving period. As in non-driven systems, the spectrum and eigenstates of the Floquet operator can be classified according to topology [2, 4, 16]. In addition to the stroboscopic evolution of the system, however, the *micromotion* that takes place within each driving period is crucial for the topological classification of periodically driven systems [17–21, 23–27].

Here we uncover the physical relationship between the micromotion of a periodically driven system and its topological invariant. We focus on two-dimensional (2D) periodically driven systems in which *all* bulk Floquet eigenstates are localized by disorder (see Fig. 1). The topological invariant of Ref. [22], computed from the system's evolution operator throughout a single driving period, distinguishes different phases of such localized systems. We show that the time-averaged magnetization density $\langle\langle m \rangle\rangle$ within a region where all states are occupied is *quantized*: $\langle\langle m \rangle\rangle = \nu/T$, where ν is the integer-valued winding number of Ref. [22] and T is the driving period. The winding number is thus related to a *bulk* experimental observable. We propose a bulk interference measurement to probe this invariant in cold atomic systems.

Topological invariants are often associated with quantized response functions in non-driven systems. Famously, the Hall *conductivity* of an insulator is proportional to the TKNN invariant, or Chern number [29]. Interestingly, topology in driven systems may directly give rise to quantization of time-averaged observables, such as the pumped *current* in the Thouless pump [30]. Similarly, the response of magnetization density to changes of chemical potential in a quantum Hall system is quantized when the chemical potential lies in an energy gap [31, 32][33]. In contrast, here we find direct quantization of the *magnetization density* itself.

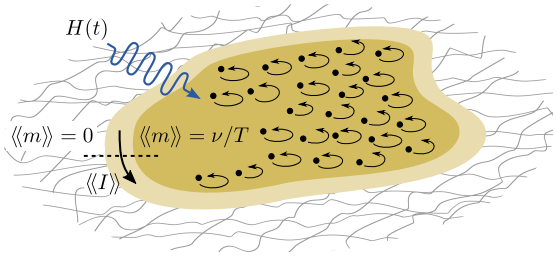

FIG. 1. Quantized magnetization density in a two-dimensional periodically driven system where all Floquet eigenstates are localized. When all sites in a region of the lattice are initially occupied (indicated by shaded area), the time-averaged magnetization density $\langle\langle m \rangle\rangle$ within the region is quantized as ν/T, where ν is an integer and T is the driving period. It follows that a quantized average current $\langle\langle I \rangle\rangle = \nu/T$ runs along the edge of the filled region.

For concreteness, we consider a periodically-driven two-dimensional lattice model with one orbital per site. Dynamics are governed by a time-periodic Hamiltonian $H(t) = H(t+T)$, where T is the driving period. The periodic driving gives rise to a unitary evolution $U(t) = \mathcal{T} e^{-i\int_0^t dt' H(t')}$, where $\mathcal{T}$ denotes time ordering. The spectrum of the Floquet operator $U(T)$, given by $U(T)|\psi_n(0)\rangle = e^{-i\varepsilon_n T}|\psi_n(0)\rangle$, defines the Floquet states $\{|\psi_n(t)\rangle\}$ and their quasienergies $\{\varepsilon_n\}$.

We characterize micromotion in Floquet states via the magnetization [34]

$$M(t) = \frac{1}{2}\left(\mathbf{r} \times \dot{\mathbf{r}}(t)\right) \cdot \hat{\mathbf{z}}, \tag{1}$$

where $\dot{\mathbf{r}}(t) = -i[\mathbf{r}, H(t)]$. In non-driven systems, the

magnetization of a state determines the response of its energy to an applied uniform magnetic field, B. In periodically driven systems, a similar relation holds between a Floquet state's time-averaged magnetization and the response of its quasienergy to an applied magnetic field. We define $\langle A\rangle_\tau \equiv \frac{1}{\tau}\int_0^\tau dt\,\langle\psi(t)|A(t)|\psi(t)\rangle$ as the time-averaged expectation value of an operator $A(t)$ in the state $|\psi(t)\rangle$. The single-period averaged magnetization of Floquet eigenstate $|\psi_n(t)\rangle$ is given by [35] (see SOM):

$$\langle M\rangle_T^{(n)} \equiv \frac{1}{T}\int_0^T dt\,\langle\psi_n(t)|M(t)|\psi_n(t)\rangle = -\frac{\partial\varepsilon_n}{\partial B}. \quad (2)$$

Using Eqs. (1) and (2), we may associate a net magnetization with a single particle in a localized Floquet eigenstate. Generalizing Eq. (2), it is useful to define a local time-averaged *magnetization density*, associated with each plaquette p of the lattice, that characterizes the response of quasienergy to a magnetic flux ϕ_p applied locally through plaquette p. We define the magnetization density operator as [36]:

$$m_p(t) = -\frac{\partial H(t)}{\partial\phi_p}, \quad \phi_p = \int_p d^2r\, B(\mathbf{r}), \quad (3)$$

where the integral is taken over the area of plaquette p.

We use the definition of magnetization density in Eq. (3) for both single particle and many-body systems. In particular, for a (single or many particle) Floquet eigenstate $|\psi(t)\rangle$ with quasienergy ε, where the density averaged over one driving period is by definition stationary, the time-averaged magnetization density is given by $\langle m_p\rangle_T = -\frac{\partial\varepsilon}{\partial\phi_p}$. By linearity, the Floquet state's time-averaged magnetization $\langle M\rangle_T$ is given by the sum of magnetization densities over all plaquettes: $\langle M\rangle_T = \sum_p \langle m_p\rangle_T a^2$, where a is the lattice constant.

In the continuum, equilibrium magnetization density is related to the current density $\mathbf{j}$ through Ampere's law, $\mathbf{j} = \nabla\times\mathbf{m}$ [37]. For a (stationary) system on the lattice, Ampere's law relates the time-averaged magnetization densities on adjacent plaquettes p and q to the time-averaged current $\langle I_{pq}\rangle_\tau$ on the bond between them [38]:

$$\langle I_{pq}\rangle_\tau = \langle m_p\rangle_\tau - \langle m_q\rangle_\tau. \quad (4)$$

In the above, we take positive current to be counterclockwise with respect to plaquette p.

Quantization of magnetization in a closed geometry.— Next, we establish the quantization of time-averaged magnetization density in a system with periodic boundary conditions (e.g., on a torus), which is completely filled with fermions. First we argue that the magnetization density in such a system must be homogeneous, with a value that can exhibit at most an exponentially-weak sensitivity on system size for large systems. We find that the value of the magnetization density in the thermodynamic limit is $\bar{m}_\infty = \nu/T$, where ν is an integer.

First, note that current must vanish in any region where all sites are either completely filled or empty. Consequently, for a fully-filled torus, all (time-averaged) bond currents vanish, $\langle I_{pq}\rangle_\tau = 0$ for all τ. According to Eq. (4), the magnetization density must therefore be the same on every plaquette. The global value of magnetization density may, however, depend on system size.

The magnetization density $\langle m_p\rangle_T$ in plaquette p is determined by the sum of contributions from all (occupied) localized Floquet states that overlap with plaquette p. If the system size is increased by adding a section of new (filled) sites in a far away region, $\langle m_p\rangle_T$ can only change by an exponentially small amount due to the contributions of the tails of the newly added localized states. We thus obtain $\langle m_p\rangle_T = \bar{m}_\infty + \mathcal{O}(e^{-L/\xi})$, where L is the linear size of the system, ξ is the single particle localization length, and $\bar{m}_\infty$ is the value in the thermodynamic limit.

Next we use Eq. (2) and spectral properties of the Floquet operator to show that the total magnetization $\langle M\rangle_T$ is quantized in the thermodynamic limit, and thus infer the quantization of $\bar{m}_\infty$. Since the net magnetic flux through a closed surface must be an integer multiple of the flux quantum, Φ_0, the strength of a uniform field B cannot be continuously varied on the torus. We therefore approximate the B-derivative in Eq. (2) by continuously varying a uniform magnetic field *locally* within the localization area of $|\psi_n(t)\rangle$, while a compensating change is made far away to keep the total flux through the torus constant. When ξ is much smaller than the system size L, the compensating field does not affect the state. This allows us to compute the contribution of each Floquet state to $\langle M\rangle_T$, up to a correction $\sim e^{-\xi/L}$.

The quantization of magnetization follows from the fact that *the sum over quasienergies of all Floquet eigenstates on the torus is unchanged, modulo $2\pi/T$, when the total magnetic flux through the torus is changed from zero to one flux quantum.* Following the arguments of Ref. [21], we consider the determinant $|U(T)|$ of the system's Floquet operator, $\log|U(T)| = \int_0^T dt\,\partial_t \log|U(t)|$. Using the identity $\partial_t \log|U(t)| = \mathrm{Tr}\left[U^\dagger(t)\partial_t U(t)\right]$, together with $\partial_t U(t) = -iH(t)U(t)$, we find [39]

$$\log|U(T)| = -i\int_0^T dt\,\mathrm{Tr}\left[H(t)\right]. \quad (5)$$

When a magnetic field is introduced, the hopping amplitudes between sites of the lattice acquire additional Peierl's phases, $H_{ab} \to H_{ab}e^{iA_{ab}}$ [40]. In the position basis, the magnetic field thus only affects the *off-diagonal* elements of the Hamiltonian, and we conclude that that $\mathrm{Tr}[H(t)]$ and hence $|U(T)|$ are independent of magnetic field. Using $|U(T)| = e^{-i\sum_n \varepsilon_n T}$, we thus find

$$\sum_n \varepsilon_n(B_0) = \sum_n \varepsilon_n(0) - \frac{2\pi\nu}{T}, \quad (6)$$

where ν is an integer and $B_0 = 2\pi/A$ is the field corresponding to one flux quantum through the torus.

When the system is large, $\varepsilon_n(B)$ is well approximated by a first-order Taylor expansion for $0 \leq B \leq B_0$. The coefficient $\partial\varepsilon_n/\partial B = -\langle M\rangle_T^{(n)}$ is the time-averaged magnetization of Floquet state n [see Eq. (2)] and

$$\varepsilon_n(B_0) = \varepsilon_n(0) - B_0\langle M\rangle_T^{(n)} + \mathcal{O}(M_0 A_n/A^2). \quad (7)$$

The correction term comes from the next order in the Taylor expansion of $\varepsilon_n(B)$, with M_0 denoting the typical scale of the time-averaged magnetization for Floquet states, and $A_n \propto \xi^2$ denoting the localization area of $|\psi_n(t)\rangle$ [41]. Above, $A = L^2$ is the area of the system.

To obtain the period-averaged magnetization density $\bar{m}_\infty$ in the thermodynamic limit, we let $A \to \infty$ and set the correction term to zero in Eq. (7). Summing over all n, and comparing with Eq. (6), we find $\langle M\rangle_T = -\sum_n[\varepsilon_n(B_0) - \varepsilon_n(0)]/B_0 = 2\pi\nu/(B_0 T)$. As discussed above, the magnetization density in any plaquette of the torus is identical and equal to $\bar{m}_\infty$ (up to corrections which are exponentially small in the system size). Using $\bar{m}_\infty = \langle M\rangle_T/A$ and $B_0 A = 2\pi$ gives

$$\langle m_p\rangle_T = \bar{m}_\infty + \mathcal{O}(e^{-L/\xi}), \quad \bar{m}_\infty = \frac{\nu}{T}. \quad (8)$$

Remarkably, this quantization has a topological origin. As we show in the SOM [38], the integer ν is equal to the winding number invariant introduced in Ref. [22]. The time-averaged magnetization density therefore serves as a bulk topological order parameter that characterizes distinct fully-localized Floquet phases.

Magnetization in finite droplets.— We now discuss the consequences of the quantized magnetization density for the experimentally relevant case of a finite droplet, where all sites in a region of linear dimension R are initially occupied (Fig. 1). Since all Floquet states are localized, the particle density will only evolve significantly in a strip of width ξ around the boundary of the filled region: the droplet retains its shape up to a smearing of its boundary. At a distance $d \gg \xi$ from this boundary, the density change remains exponentially small in d/ξ at any time.

In the situation described here, where the system is not in a Floquet eigenstate, the particle density is not strictly stationary over a single period. However, the fact that the occupation on any site is bounded between zero and one implies that $\lim_{\tau\to\infty}\langle\dot{\rho}\rangle_\tau = 0$. Therefore the long time averaged magnetization density, $\langle\langle m_p\rangle\rangle \equiv \lim_{\tau\to\infty}\langle m_p\rangle_\tau$, is gauge invariant [36] and obeys Ampere's law, Eq. (4). Deep inside the filled region, all (localized) Floquet states are occupied with probabilities exponentially close to one and $\langle\langle m_p\rangle\rangle$ attains the quantized value $\bar{m}_\infty$, as on the torus, up to an exponentially small correction: $\langle\langle m_{\rm in}\rangle\rangle = \bar{m}_\infty + \mathcal{O}(e^{-R/\xi})$. (The correction follows from similar reasoning as used above.)

Interestingly, Ampere's law dictates that the filled region should exhibit a quantized current circulating around its boundary [42]. As argued above, in a phase where $\bar{m}_\infty \neq 0$, the magnetization density $\langle\langle m_p\rangle\rangle$ in the interior of the droplet (at a distance $\ell \gg \xi$ from the boundary) must be given by the quantized value $\bar{m}_\infty$. The magnetization density must then drop to zero over a distance of order ξ across the boundary of the initially filled region. According to Eq. (4), the long-time averaged bond current is only significant within the same strip of width ξ around the boundary of the initially filled region. It furthermore follows that the total time-averaged current $\langle\langle I\rangle\rangle$ passing through a cut through this strip (e.g., the cut shown in Fig. 1), is given by:

$$\langle\langle I\rangle\rangle = \bar{m}_\infty + \mathcal{O}(e^{-R/\xi}). \quad (9)$$

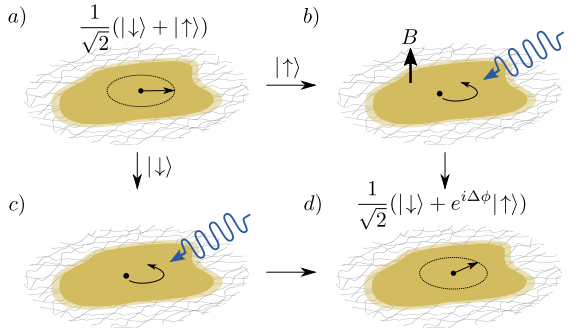

FIG. 2. Interferometric measurement of quantized magnetization in a cold-atom system. a) The system is prepared by filling a region of an optical lattice with spin-1/2 atoms fully polarized along x. b,c) The system is evolved with a spin-independent periodic driving Hamiltonian, plus a weak spin-dependent uniform synthetic magnetic field. d) The spin-dependent field gives rise to a phase-difference $\Delta\phi$ between the $|\uparrow\rangle$ and $|\downarrow\rangle$ components of each atom's wavefunction. The phase shift yields a net y-polarization of total spin, proportional to the system's time-averaged magnetization.

The fact that the filled droplet retains its shape implies the quantization of the droplet's *spatially averaged* magnetization density, $\langle\langle\overline{m}\rangle\rangle \equiv \langle\langle M\rangle\rangle/A_{\rm filled}$, where $\langle\langle M\rangle\rangle = \sum_p \langle\langle m_p\rangle\rangle a^2$ and $A_{\rm filled} \sim R^2$ is the area of the filled region. Since the magnetization density gradually drops to zero in a region of width $\sim \xi$ around the boundary of the droplet, $A_{\rm filled}$ is uncertain, and $\langle\langle\overline{m}\rangle\rangle$ is only quantized up to a power-law correction $\langle\langle\overline{m}\rangle\rangle = \bar{m}_\infty + \mathcal{O}(\xi/R)$. We now show how to experimentally access the spatially averaged magnetization density $\langle\langle\overline{m}\rangle\rangle$, thereby offering a direct probe to measure the bulk topological invariant of the anomalous Floquet Anderson insulator (AFAI).

Interferometric probe of quantized magnetization.— We now outline an interferometric scheme for measuring the orbital magnetization of a cloud of cold atoms in an optical lattice (see Fig. 2). Consider an atom traversing a closed trajectory in the presence of a weak magnetic field B. Semiclassically, the wave-function picks up an additional phase shift $\Delta\phi = BA$ due to the field, where A is the area enclosed by the orbit [43]. Correspondingly, a simple quantum mechanical calculation [38] shows that the phase shift acquired by an atom in Floquet state

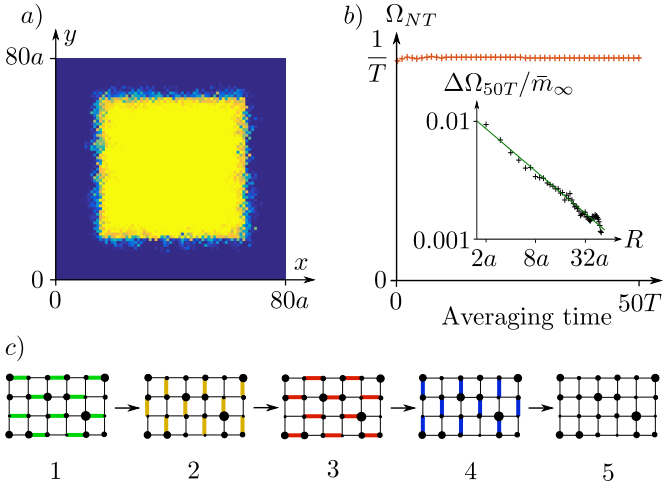

FIG. 3. a) Particle density in the system after 20 driving periods, for an initially filled 50×50 square of sites. b) Normalized growth rate Ω_{NT} of the average y-spin per atom (see text above Eq. (10). The long-time-averaged magnetization density $\langle\langle \overline{m} \rangle\rangle$ is extracted from the saturation value at long times. *Inset*: Deviation $\Delta\Omega_{50T}$ of Ω_{50T} from the quantized value $\bar{m}_\infty$ *vs.* droplet size R. The value of $\Delta\Omega_{50T}$ is obtained as an RMS average of $\Omega_{50T} - \bar{m}_\infty$ over 100 disorder realizations. c) Depiction of the tight-binding model.

$|\psi_n(t)\rangle$ over a full driving period is proportional to the state's magnetization, $\Delta\phi_n = \langle M \rangle_T^{(n)} BT$.

Using the phase shift described above, the magnetization of a cloud of atoms can be measured in a Ramsey-type interference experiment in a situation where the atoms have two internal ("spin") states $|\uparrow\rangle$ and $|\downarrow\rangle$, and where a spin dependent magnetic field can be applied. First, the system should be prepared by completely filling a region of known area, A_{filled}, with atoms fully spin-polarized along the "x"-direction, $|\psi(0)\rangle \propto (|\uparrow\rangle + |\downarrow\rangle)/\sqrt{2}$, (Fig. 2a). The system should then be evolved with the (field free) driving Hamiltonian to allow the particle density to reach a steady profile [44], as in Fig. 3a. To perform the measurement, the cloud of atoms is then evolved through N driving periods in the presence of a weak spin-dependent orbital effective magnetic field B (Figs. 2bc), which, e.g., acts only on the $|\uparrow\rangle$ species. Through the evolution, the $|\uparrow\rangle$ component of each atom's wave function gains a phase shift relative to the $|\downarrow\rangle$ component, yielding a nonzero average y-spin per particle, $\langle \overline{\sigma}_y \rangle$, (Fig. 2d). For small precession angles, the average y-spin after N periods is given by $\langle \overline{\sigma}_y(NT) \rangle \equiv \Omega_{NT} B a^2 NT$, with [38]

$$\Omega_{NT} = \langle\langle \overline{m} \rangle\rangle + \frac{1}{NT} \mathcal{O}\left(\frac{\xi^{3/2}}{a R^{1/2}} \right) + \mathcal{O}(B). \qquad (10)$$

Importantly, the second term vanishes in the long time limit (and scales to zero at finite times for large systems), thus revealing the quantized magnetization density [38].

Numerical results.— We simulated the experimental protocol outlined above using a tight-binding model on a two-dimensional bipartite square lattice, with Hamiltonian $H(t) = H_{\text{clean}}(t) + V_{\text{disorder}}$. The Hamiltonian $H_{\text{clean}}(t)$ was considered in Ref. [17], and is of the form

$$H_{\text{clean}}(t) = \sum_{\mathbf{r} \in A} \sum_{n=1}^{4} J_n(t) (c^\dagger_{\mathbf{r}+\mathbf{b}_n} c_{\mathbf{r}} + h.c.), \qquad (11)$$

where $c_{\mathbf{r}}$ is the fermionic annihilation operator on the lattice site with coordinate $\mathbf{r}$, and the first sum runs over sites $\mathbf{r}$ on sublattice A. The vectors $\{\mathbf{b}_n\}$ are given by $\mathbf{b}_1 = -\mathbf{b}_3 = (a, 0)$ and $\mathbf{b}_2 = -\mathbf{b}_4 = (0, a)$, where a is the lattice constant. The driving period is divided into five segments of equal length $T/5$. In the nth segment ($n \leq 4$), $J_n(t) = J$, while all other hopping amplitudes are set to zero; in the 5th segment all hopping amplitudes are set to zero (see Fig. 3c). We introduce disorder through a time-independent potential $V_{\text{disorder}} = \sum_{\mathbf{r}} w_{\mathbf{r}} c^\dagger_{\mathbf{r}} c_{\mathbf{r}}$, where the sum now runs over all sites, and the on-site energies $\{w_{\mathbf{r}}\}$ are randomly drawn from a uniform distribution in the interval $[-V, V]$. The model has hopping amplitude J and disorder strength V both set to $2.5\pi/T$, which brings the system well into the fully-localized phase [38].

To find the magnetization density of the system, we consider a single disorder realization on a lattice of 80×80 sites and open boundary conditions. We initially fill a region of 50×50 sites (i.e., $R = 50$) centered in the middle of the lattice, and prepare the state by evolving it for 20 driving periods at zero magnetic field (see Fig. 3a). For further times ranging from 0 to $50T$ we evolve the system in the presence of a spin-dependent magnetic field of strength $Ba^2 = 2\pi \cdot 10^{-4}$, corresponding to approximately 1 flux quantum through the system [38]. We extract the spatially averaged magnetization density $\langle\langle \overline{m} \rangle\rangle$ from the long-time limit of the normalized growth rate Ω_{NT} of average y-spin per atom, $\langle \overline{\sigma}_y(NT) \rangle$. As expected, Ω_{NT} rapidly converges (up to a finite-size correction) to the quantized value of the magnetization density, $1/T$, reaching 0.9998 after 100 periods (Fig. 3b). We repeated this simulation for multiple disorder realizations and for various sizes of the droplet (see SOM for additional data). The inset in Fig. 3b shows the deviation of Ω_{50T} from the quantized value $\bar{m}_\infty = 1/T$ for various sizes of the droplet, taken as a root-mean-square average over 100 disorder realizations at each system size. We find a power law decay of the fluctuations with system size, $\Delta\Omega_{50T} \sim R^{-\alpha}$, with $\alpha = 0.55$.

Discussion.— Here we showed that the topological invariant of the AFAI is directly related to a bulk physical observable, the magnetization density. We then proposed an experimental scheme for measuring the quantized magnetization density in cold atomic systems.

We have derived the quantization of magnetization density within a tight-binding model with one (s-type) orbital per site. In particular, this means that each on-site orbital does not carry any intrinsic magnetization. In the continuum, small non-quantized contributions to

the magnetization density may arise due to mixing with higher bands. However, such contributions are strongly suppressed when the driving is adiabatic with respect to the gap to higher bands, and the lattice is very deep such that the gap is large compared to the bandwidth [45].

It is natural to expect that our results will hold also in the presence of interactions, given that the system is strongly disordered and therefore may be many-body localized. Exploring the interacting regime of the AFAI phase is an interesting direction of ongoing study [46, 47].

M.R. gratefully acknowledges the Villum Foundation and the People Programme (Marie Curie Actions) of the European Unions Seventh Framework Programme (FP7/2007-2013) under REA grant agreement PIIF-GA-2013-627838 for support. N.L. and E.B. acknowledge financial support from the European Research Council (ERC) under the European Unions Horizon 2020 research and innovation programme (grant agreement No 639172). G. R. is grateful for support from the NSF through Grant No. DMR-1410435, the Institute of Quantum Information and Matter, an NSF Frontier center funded by the Gordon and Betty Moore Foundation, and the Packard Foundation, and further thanks the Aspen Center for Physics for their hospitality.

[1] W. Yao, A. H. MacDonald, and Q. Niu, Phys. Rev. Lett. **99**, 047401 (2007).
[2] T. Oka and H. Aoki, Phys. Rev. B **79**, 081406 (2009).
[3] J.-i. Inoue and A. Tanaka, Phys. Rev. Lett. **105**, 017401 (2010).
[4] N. H. Lindner, G. Refael, and V. Galitski, Nat. Phys. **7**, 490 (2011).
[5] N. H. Lindner, D. L. Bergman, G. Refael, and V. Galitski, Phys. Rev. B **87**, 235131 (2013).
[6] Z. Gu, H. A. Fertig, D. P. Arovas, and A. Auerbach, Phys. Rev. Lett. **107**, 216601 (2011).
[7] T. Kitagawa, T. Oka, A. Brataas, L. Fu, and E. Demler, Phys. Rev. B **84**, 235108 (2011).
[8] P. Delplace, A. Gomez-Leon, and G. Platero, Phys. Rev. B **88**, 245422 (2013).
[9] Y. T. Katan and D. Podolsky, Phys. Rev. Lett. **110**, 016802 (2013).
[10] M. Lababidi, I. I. Satija, and E. Zhao, Phys. Rev. Lett. **112**, 026805 (2014).
[11] T. Iadecola, D. Campbell, C. Chamon, C.-Y. Hou, R. Jackiw, S.-Y. Pi, and S. V. Kusminskiy, Phys. Rev. Lett. **110**, 176603 (2013).
[12] N. Goldman and J. Dalibard, Phys. Rev. X **4**, 031027 (2014).
[13] A. G. Grushin, A. Gómez-León, and T. Neupert, Phys. Rev. Lett. **112**, 156801 (2014).
[14] A. Kundu, H. Fertig, and B. Seradjeh, Phys. Rev. Lett. **113**, 236803 (2014).
[15] P. Titum, N. H. Lindner, M. C. Rechtsman, and G. Refael, Phys. Rev. Lett. **114**, 056801 (2015).
[16] T. Kitagawa, E. Berg, M. Rudner, and E. Demler, Phys. Rev. B **82**, 235114 (2010).
[17] M. S. Rudner, N. H. Lindner, E. Berg, and M. Levin, Phys. Rev. X **3**, 031005 (2013).
[18] L. Jiang, T. Kitagawa, J. Alicea, A. R. Akhmerov, D. Pekker, G. Refael, J. I. Cirac, E. Demler, M. D. Lukin, and P. Zoller, Phys. Rev. Lett. **106**, 220402 (2011).
[19] J. K. Asboth, B. Tarasinski, and P. Delplace, Phys. Rev. B **90**, 125143 (2014).
[20] D. Carpentier, P. Delplace, M. Fruchart, and K. Gawedzki, Phys. Rev. Lett. **114**, 106806 (2015).
[21] F. Nathan and M. S. Rudner, New Journal of Physics **17**, 125014 (2015).
[22] P. Titum, E. Berg, M. S. Rudner, G. Refael, and N. H. Lindner, Phys. Rev. X **6**, 021013 (2016).
[23] R. Roy and F. Harper, arXiv:1602.08089 (2016).
[24] D. V. Else and C. Nayak, Phys. Rev. B **93**, 201103 (2016).
[25] C. W. von Keyserlingk and S. L. Sondhi, Phys. Rev. B **93**, 245145 (2016).
[26] A. C. Potter, T. Morimoto, and A. Vishwanath, arXiv:1602.1602.05194 (2016).
[27] R. Roy and F. Harper, arXiv:1603.06944 (2016).
[28] D. V. Else, B. Bauer, and C. Nayak, arXiv:1603.08001 (2016).
[29] D. J. Thouless, M. Kohmoto, M. P. Nightingale, and M. den Nijs, Phys. Rev. Lett. **49**, 405 (1982).
[30] D. J. Thouless, Phys. Rev. B. **27**, 6083 (1983).
[31] A. H. Macdonald, *Quantum coherence in mesoscopic systems* (Springer, 1991), ISBN 978-0-306-43889-9.
[32] S. A. J. Wiegers, M. Specht, L. P. Lévy, M. Y. Simmons, D. A. Ritchie, A. Cavanna, B. Etienne, G. Martinez, and P. Wyder, Phys. Rev. Lett. **79**, 3238 (1997).
[33] This can be seen from the fact that, within the quantum Hall effect, this response function is related to the Hall conductivity by the Streda formula [48].
[34] The magnetization, Eq. (1), is independent of shifts of origin $\mathbf{r} \to (\mathbf{r} - \mathbf{r}_0)$ when evaluated in stationary states with $\langle \dot{\mathbf{r}} \rangle = 0$. In a fully localized system, this implies that the magnetization of a Floquet state averaged over an integer number of driving periods, or the long-time average for a generic intial state, is origin-independent.
[35] Note that we measure magnetic field in units of [1/Area], such that the Aharonov-Bohm phase of a closed trajectory is equal to the flux enclosed by the path.
[36] The operator $m_p(t)$ in Eq. (3) requires a gauge specification in order to be uniquely defined. However, expectation values of m_p are *gauge-independent* when averaged over any time window τ over which the particle density is stationary $\langle \dot{\rho} \rangle_\tau = 0$, see SOM for details.
[37] In this case, the magnetization density is also only well-defined when the charge density is stationary $\nabla \cdot \mathbf{j} = 0$.
[38] See supplementary online information.
[39] Here we choose $\log|U(t)|$ to be continuous, with $\log|U(0)| = 0$.
[40] Note that it is only possible to modify the Hamiltonian in this way when the the total flux through the torus is an integer multiple of ϕ_0, see discussion above Eq. (5).
[41] The magnetization $\langle M \rangle_T^{(n)}(B)$ of a Floquet eigenstate $|\psi_n\rangle$ is only significantly affected by the magnetic field when the flux through the localization area A_n of $|\psi_n\rangle$ becomes comparable to the flux quantum. Thus we write $-\frac{\partial \varepsilon_n}{\partial B} = \langle M \rangle^{(n)}(0) + \mathcal{O}(BA_nM_0)$, where $M_0 \sim \frac{\partial M}{\partial (BA_n)}$ is comparable to the magnetization of $|\psi_n\rangle$.
[42] The current $\langle\langle I \rangle\rangle$ flows around the droplet boundary, in

the *bulk* of the lattice, where all states are localized (i.e., not at a physical edge where chiral edge states reside).
[43] More precisely, the overlap between the wave functions evolved with and without the magnetic field given by $1 - i\Delta\phi$ to first order in the field B.
[44] This initial evolution step minimizes systematic transients due to the sharp boundary, see SOM.
[45] In this limit, over one driving period the center of mass of the orbital on each site shifts by a distance that is small compared with the lattice spacing. The non-quantized contribution to the magnetization density (in units of the driving frequency) is proportional to the area swept out by the center of mass, divided by the area of the unit cell, and is therefore small compared to $\bar{m}_\infty = 1/T$ in the AFAI phase.
[46] H. C. Po, L. Fidkowski, T. Morimoto, A. C. Potter, and A. Vishwanath, arXiv:1609.00006 (2016).
[47] F. Harper and R. Roy, arXiv:1609.06303 (2016).
[48] P. Streda, Journal of Physics C: Solid State Physics **15**, L717 (1982).

Supplementary Material: Quantized magnetization density in periodically driven systems

Magnetization as the response of quasienergy to a magnetic field

Here we derive Eq. (2) in the main text, showing that the single-period averaged magnetization $\langle M\rangle_T^{(n)}$ of a Floquet state $|\psi_n\rangle$ with quasienergy ε_n is given by the response of its quasienergy to an applied "probing" uniform magnetic field, B: $\langle M\rangle_T^{(n)} = -\frac{\partial\varepsilon_n}{\partial B}$. (Note that, in addition to the probing field B, a nontrivial field $B_0(\mathbf{r},t)$ may already be present in the system.) Throughout this work the magnetic field is given in units of [1/Area], such that the flux quantum has value 2π.

As a first step, we note that $\frac{\partial\varepsilon_n}{\partial B}$ can be written as

$$\frac{\partial\varepsilon_n}{\partial B} = \frac{i}{T}\langle\psi_n|\left(U^\dagger(T)\frac{\partial}{\partial B}U(T)\right)|\psi_n\rangle. \tag{S1}$$

This relation can be checked using the spectral decomposition $U(T) = \sum_n |\psi_n\rangle\langle\psi_n|e^{-i\varepsilon_n T}$, together with the identity $\langle\psi_n|\frac{\partial}{\partial B}|\psi_n\rangle + \frac{\partial}{\partial B}\big[\langle\psi_n|\big]|\psi_n\rangle = 0$. Here $\frac{\partial}{\partial B}|\psi_n\rangle$ measures the change of Floquet state $|\psi_n\rangle$ when a uniform magnetic field B is introduced to the system.

We now use $U(T) = \mathcal{T}e^{-i\int_0^T dtH(t)}$ to obtain

$$U^\dagger(T)\frac{\partial}{\partial B}U(T) = -i\int_0^T dt\, U^\dagger(t)\frac{\partial H(t)}{\partial B}U(t). \tag{S2}$$

Hence, substituting back into Eq. (S1), we get

$$\frac{\partial\varepsilon_n}{\partial B} = \frac{1}{T}\int_0^T \langle\psi_n(t)|\frac{\partial H(t)}{\partial B}|\psi_n(t)\rangle, \tag{S3}$$

where $|\psi_n(t)\rangle = U(t)|\psi_n\rangle$ is the time-evolved Floquet eigenstate at time t.

What is the nature of the operator $\frac{\partial H}{\partial B}$? By analogy to equilibrium systems, clearly it is suggestive of magnetization. However, similar to the magnetization density operator m_p discussed in the main text, the operator $\frac{\partial H}{\partial B}$ is gauge-dependent. Nonetheless, expectation values of $\frac{\partial H}{\partial B}$ taken in *stationary states* are in fact gauge invariant, and therefore physical (see next section). The stationarity condition is satisfied for the full-period average of $\frac{\partial H}{\partial B}$ in a Floquet state, as appears on the right hand side of Eq. (S3). Indeed this must be the case, since the quantity $\frac{\partial\varepsilon_n}{\partial B}$ on the left hand side is itself gauge-invariant.

To obtain an expression for $\frac{\partial H(t)}{\partial B}$, we consider the change of the Hamiltonian when the small uniform probing magnetic field B is introduced. In this case, the matrix elements $H_{ab}(t)$ of the Hamiltonian in the lattice site basis (here a, b refer to lattice site indices) acquire Peierl's phases: $H_{ab}(t) \to H_{ab}(t)e^{i\int_{\mathbf{r}_b}^{\mathbf{r}_a} d\mathbf{r}\cdot\mathbf{A}(\mathbf{r})}$, where the contour of integration is a straight line from site b to site a and $\mathbf{B} = \nabla\times\mathbf{A}$. Given that the result of Eq. (S3) is gauge-independent, we work in the symmetric gauge below. This gauge choice highlights the direct relation to the magnetization defined in Eq. (1) of the main text. In the symmetric gauge, a uniform perpendicular "probing" magnetic field B is produced by the vector potential $\mathbf{A}(\mathbf{r}) = \frac{B}{2}\hat{\mathbf{z}}\times\mathbf{r}$. Using the identity $A\cdot(B\times C) = B\cdot(C\times A)$, we thus obtain the following modification of $H_{ab}(t)$ due to the probe field B :

$$\begin{aligned} H_{ab}(t) &\to H_{ab}(t)\exp\left[\frac{iB}{2}\int_{\mathbf{r}_b}^{\mathbf{r}_a} d\mathbf{r}\cdot(\hat{\mathbf{z}}\times\mathbf{r})\right] \\ &= H_{ab}(t)\exp\left[\frac{iB}{2}\hat{\mathbf{z}}\cdot\left(\int_{\mathbf{r}_b}^{\mathbf{r}_a}\mathbf{r}\times d\mathbf{r}\right)\right] \\ &= H_{ab}(t)\exp\left[\frac{iB}{2}\hat{\mathbf{z}}\cdot(\mathbf{r}_a\times(\mathbf{r}_a-\mathbf{r}_b))\right]. \end{aligned}$$

Here we used that $\mathbf{r}_a\times(\mathbf{r}_a-\mathbf{r}_b) = \mathbf{r}_b\times(\mathbf{r}_a-\mathbf{r}_b)$.

Taking the derivative of $H_{ab}(t)$ with respect to the probe field strength B, we obtain

$$\frac{\partial H_{ab}(t)}{\partial B} = \frac{i}{2}H_{ab}(t)\,(\mathbf{r}_a\times(\mathbf{r}_a-\mathbf{r}_b))\cdot\hat{\mathbf{z}}. \tag{S4}$$

This structure of the matrix elements of H implies that

$$\frac{\partial H(t)}{\partial B} = \frac{i}{2}\,(\mathbf{r}\times[\mathbf{r},H(t)])\cdot\hat{\mathbf{z}}. \tag{S5}$$

Equation (S5) can be verified by taking a matrix element with $\langle a|$ and $|b\rangle$ on the left and right, respectively, and comparing with Eq. (S4). Comparing with Eq. (1) of the main text, and using $\dot{\mathbf{r}}(t) = -i[\mathbf{r},H]$, we identify the right hand side above as minus the magnetization, $-M(t)$. Substituting this result into Eq. (S3), we obtain Eq. (2) in the main text.

Gauge invariance of magnetization density

Here we show that the magnetization density operator $m_p(t)$, defined in Eq. (3) of the main text, yields gauge-independent time-averaged expectation values if and only if the density is stationary over the averaging interval τ, i.e., $\langle\dot{\rho}\rangle_\tau = 0$. In this case, we furthermore show that the magnetization density obeys the lattice version of Ampere's law given in Eq. (4) of the main text.

In the presence of a magnetic flux ϕ_p piercing through plaquette p, the matrix elements of the Hamiltonian in the lattice site basis are given by $H_{ab}(\phi_p) = e^{iA_{ab}(\phi_p)}H_{ab}(\phi_p = 0)$. (Here we work in units where the lattice constant is 1). Here the vector potential $\{A_{ab}(\phi_p)\}$ should have the following property: for a sequence of sites $(a_1, a_2, \ldots a_N)$ forming a closed counterclockwise loop on the lattice, the phase

$\sum_{n=1}^{N} A_{a_{n+1}a_n}(\phi_p)$ should equal ϕ_p if the loop encloses the plaquette p, while the sum should vanish otherwise (here we set $a_{N+1} = a_1$). The magnetization density operator is then given by

$$m_p(t) = -\frac{\partial H(t)}{\partial \phi_p} = -\sum_{\langle a,b\rangle} \frac{\partial H(t)}{\partial A_{ab}} \frac{\partial A_{ab}}{\partial \phi_p}, \qquad \text{(S6)}$$

where the sum runs over all pairs of sites on the lattice connected by bonds.

We note that there is a gauge freedom in choosing $A_{ab}(\phi_p)$: if the vector potential $\{A_{ab}(\phi_p)\}$ results in a flux ϕ_p on plaquette p, then so will a vector potential $\{A'_{ab}(\phi_p)\}$ that satisfies

$$A'_{ab}(\phi_p) = A_{ab}(\phi_p) + f_a(\phi_p) - f_b(\phi_p), \qquad \text{(S7)}$$

where $\{f_a(\phi)\}$ can be any set of scalar functions.

In order for $\langle m_p\rangle_\tau$ to be gauge-invariant, the time-averaged expectation value of the right hand side of Eq. (S6) should remain unchanged if we replace A_{ab} with A'_{ab}. In order for this to be satisfied, we must have

$$\sum_{\langle a,b\rangle} \left\langle \frac{\partial H}{\partial A_{ab}} \right\rangle_\tau (g_a - g_b) = 0, \qquad \text{(S8)}$$

where $\{g_a = \frac{\partial f_a}{\partial \phi}\big|_{\phi=0}\}$ are arbitrary coefficients. Equation (S8) is satisfied if we require that the net current flowing into or out of every site a on the lattice vanishes:

$$\sum_{b\in \text{n.n.}(a)} \langle I_{ab}\rangle_\tau = 0, \quad I_{ab}(t) = -\frac{\partial H(t)}{\partial A_{ab}}. \qquad \text{(S9)}$$

Here the sum runs over all sites b that are connected with a bond to site a. It is trivial to see that this condition ensures that the sum over terms proportional to g_a in Eq. (S8) vanishes. The vanishing of the sum over terms proportional to g_b follows by relabeling.

The sum on the left hand side of Eq. (S9) gives the net current flowing into site a, which is equal to the rate of change of density: $\sum_{b\in\text{n.n.}(a)} I_{ab} = \dot{\rho}_a$, where ρ_a is the density operator on site a. Therefore the gauge invariance condition for expectation values of the magnetization density, Eq. (S8), is satisfied if and only if the density on every site is stationary over the time-window from 0 to τ: $\langle \dot{\rho}_a\rangle_\tau = 0$. This condition is the lattice-analogue of the condition that the current density in the continuum must be divergence-free.

Ampere's law on the lattice

To prove the lattice version of Ampere's law, we first consider the case where the vector potential is given by A_{ab} on a single bond ab, in the direction from site b to site a, and zero everywhere else. In this situation the magnetic flux is zero everywhere, except for the two plaquettes p and q adjacent to the bond ab, here taken such that the direction from site b to site a is counterclockwise with respect to plaquette p. In these two neighboring plaquettes, the fluxes are given by $\phi_p = A_{ab}$ and $\phi_q = -A_{ab}$, respectively. Hence, with this choice of gauge (i.e., A nonzero on a single bond),

$$\frac{\partial H(t)}{\partial A_{ab}} = \frac{\partial H(t)}{\partial \phi_p} - \frac{\partial H(t)}{\partial \phi_q}. \qquad \text{(S10)}$$

Noting that $\frac{\partial H(t)}{\partial A_{ab}} = -I_{ab}(t)$, and $m_p = -\frac{\partial H(t)}{\partial \phi_p}$, we obtain an operator equation similar to Eq. (4) in the main text. However, this *operator equation* holds only in the specific gauge above, where A is nonzero only on the bond ab. Importantly, as shown above, the *time-averaged expectation value* of the right hand side is gauge-independent for times τ where the density is stationary, $\langle\dot{\rho}\rangle_\tau = 0$. Therefore Eq. (S10) produces meaningful physical results, and reduces to Eq. (4) of the main text, when it is used to compute time-averaged expectation values in stationary states.

Relation to winding number

Here we show that the quantized value of the magnetization density for a fully-localized Floquet system on a torus, $\bar{m}_\infty$, is a topological invariant; its value is equal to $W[U]/T$, where $W[U]$ is the winding number introduced in Ref. S1. Noting that the numbers $W[U]$ and $\bar{m}_\infty$ do not change when we increase the system size, provided that all Floquet states remain localized, we will consider the limit where the size L goes to infinity. In this section, we work in the Heisenberg picture.

In order to define the winding number $W[U]$, we consider the Hamiltonian $H(\mathbf{A}, t)$ of the system when a uniform vector potential $\mathbf{A}$ is introduced along the surface of the torus. Let $U(\mathbf{A}, t)$ be the corresponding evolution operator of the system. As an important ingredient in the computation of the winding number, we first define the effective Hamiltonian of the system, $H_{\text{eff},\varepsilon}(\mathbf{A})$, via: $U(\mathbf{A}, T) = e^{-iH_{\text{eff},\varepsilon}(\mathbf{A})T}$, where the eigenvalues of $H_{\text{eff},\varepsilon}(\mathbf{A})$ lie in the interval $[\varepsilon, \varepsilon+2\pi/T)$. Here ε is chosen within one of the system's quasienergy gaps, which are present due to the finite extent of the system for any fixed L (see Ref. S1). To find the system's winding number, we define the $2T$-periodic evolution $\tilde{U}_\varepsilon(\mathbf{A}, t)$, obtained by first evolving the system with Hamiltonian $H(\mathbf{A}, t)$ in the time-interval $[0, T]$, and then applying a static Hamiltonian $-H_{\text{eff},\varepsilon}(\mathbf{A})$ in the time-interval $[T, 2T]$. The evolution operator $\tilde{U}_\varepsilon(\mathbf{A}, t)$ is given by $U(\mathbf{A}, t)$ in the first half of the driving, from 0 to T, and by $e^{-iH_{\text{eff},\varepsilon}(\mathbf{A})(2T-t)}$ in the second half of the driving. In particular, the extended evolution satisfies $\tilde{U}_\varepsilon(\mathbf{A}, 2T) = 1$.

With the definition of $\tilde{U}_\varepsilon(\mathbf{A},t)$ above, we obtain the winding number of the evolution via:

$$W[U] = \frac{1}{8\pi^2}\int_0^{2T} dt \int_0^{2\pi/L} d^2\mathbf{A} \\ \mathrm{Tr}\left(\tilde{U}^\dagger\partial_t\tilde{U}\cdot\tilde{U}^\dagger\partial_{A_x}\tilde{U}\cdot\tilde{U}^\dagger\partial_{A_y}\tilde{U}\right) - x\leftrightarrow y. \tag{S11}$$

Given that W is independent of ε (see Ref. S1), for brevity we drop the subscript ε on $\tilde{U}$ here and below.

As a first step in our derivation, we rewrite the above formula using basic identities for the time-evolution operator. We first use the identities $\partial_t\tilde{U} = -i\tilde{H}\tilde{U}$ and $\partial_{A_x}\tilde{U}\cdot\tilde{U}^\dagger = -\tilde{U}\partial_{A_x}\tilde{U}^\dagger$ to obtain

$$W[U] = \frac{i\varepsilon_{\alpha\beta}}{8\pi^2}\int_0^{2T} dt \int_0^{2\pi/L} d^2\mathbf{A}\,\mathrm{Tr}\left(\tilde{H}\partial_{A_\alpha}\tilde{U}\cdot\partial_{A_\beta}\tilde{U}^\dagger\right).$$

Here $\varepsilon_{\alpha\beta}$ is the antisymmetric tensor, with $\alpha,\beta=\{x,y\}$. Next, we perform partial integration over A_α and obtain

$$W[U] = \frac{i\varepsilon_{\alpha\beta}}{8\pi^2}\int_0^{2T} dt \left[\int_0^{2\pi/L} dA_\beta \mathrm{Tr}\left(\tilde{H}\tilde{U}\cdot\partial_{A_\beta}\tilde{U}^\dagger\right)_{A_\alpha=0}^{A_\alpha=2\pi/L} \\ - \int_0^{2\pi/L} d^2\mathbf{A}\,\mathrm{Tr}\left(\partial_{A_\alpha}\tilde{H}\tilde{U}\cdot\partial_{A_\beta}\tilde{U}^\dagger\right)\right]. \tag{S12}$$

We now make use of the fact that we can write $\tilde{H}(\mathbf{A}+\hat{\mathbf{e}}_\alpha 2\pi/L,t) = X_\alpha^\dagger\tilde{H}(\mathbf{A},t)X_\alpha$, where $\hat{\mathbf{e}}_\alpha$ is the α-unit vector, and $X_\alpha = e^{2\pi i x_\alpha/L}$ (see Ref. S1 for more details). Similarly, $\tilde{U}(\mathbf{A}+\hat{\mathbf{e}}_\alpha 2\pi/L,t) = X_\alpha^\dagger\tilde{U}(\mathbf{A},t)X_\alpha$. Using that $\partial_{A_\beta}X_\alpha = 0$ when $\alpha\neq\beta$, together with the cyclic property of the trace, we obtain

$$\mathrm{Tr}\left(\tilde{H}\tilde{U}\cdot\partial_{A_\beta}\tilde{U}^\dagger\right)_{\mathbf{A}=\left(\frac{2\pi}{L},A_\beta\right)} = \mathrm{Tr}\left(\tilde{H}\tilde{U}\cdot\partial_{A_\beta}\tilde{U}^\dagger\right)_{\mathbf{A}=(0,A_\beta)}.$$

Hence the integrand in the first term in Eq. (S12) vanishes, and

$$W[U] = \frac{-i\varepsilon_{\alpha\beta}}{8\pi^2}\int_0^{2T} dt \int_0^{2\pi/L} d^2\mathbf{A}\,\mathrm{Tr}\left(\partial_{A_\alpha}\tilde{H}\cdot\tilde{U}\partial_{A_\beta}\tilde{U}^\dagger\right). \tag{S13}$$

Using the identity $\partial_{A_\beta}\tilde{U}^\dagger = -\tilde{U}^\dagger\partial_{A_\beta}\tilde{U}\tilde{U}^\dagger$, along with the cyclic property of the trace, we get

$$W[U] = \frac{i}{8\pi^2}\int_0^{2T} dt \int_0^{2\pi/L} d^2\mathbf{A}\,\mathrm{Tr}\left(\tilde{U}^\dagger\partial_{A_\alpha}\tilde{H}\tilde{U}\cdot\tilde{U}^\dagger\partial_{A_\beta}\tilde{U}\right).$$

Going to the thermodynamic limit $L\to\infty$, we treat the integrand as constant within the $\mathbf{A}$-interval $[0,2\pi/L]$ (cf. Ref. S2). Thus we arrive at the formula

$$W[U] = \frac{i}{2L^2}\int_0^{2T} dt\,\mathrm{Tr}\left(\tilde{U}^\dagger\left(\partial_{A_\alpha}\tilde{H}\right)\tilde{U}\cdot\tilde{U}^\dagger\partial_{A_\beta}\tilde{U}\right). \tag{S14}$$

What we have achieved so far, with Eq. (S14), is to relate the winding number to two Heisenberg picture operators, $\tilde{U}^\dagger\partial_{\mathbf{A}}\tilde{U}$, and $\tilde{U}^\dagger\left(\partial_{\mathbf{A}}\tilde{H}\right)\tilde{U}$. Below we expose the physical meaning of each of these operators, and thereby link the winding number to the system's magnetization.

Displacement operator

Having transformed the original winding number formula (S11) into the form of Eq. (S14), we now introduce an additional operator that will be useful in making the final connection with the magnetization. Specifically, for a system with Hamiltonian $H(t)$, and evolution $U(t)$, we introduce the "displacement operator" $\Delta\mathbf{r}(t)$:

$$\Delta\mathbf{r}(t) \equiv -iU^\dagger(t)\partial_{\mathbf{A}}U(t). \tag{S15}$$

With this definition, we note that $\partial_t\Delta\mathbf{r}(t) = U^\dagger(t)\left(-\partial_{\mathbf{A}}H(t)\right)U(t)$. The displacement operator can be seen as the Heisenberg picture operator that measures the displacement of a particle relative to its starting point, in the sense that displacement is the time-integral of the velocity. This definition is important because the standard position operator on the torus is complicated by the necessity of imposing a branch cut due to the periodic boundary conditions. The displacement operator in Eq. (S15) is insensitive to this issue.

To further elucidate the physical meaning of the displacement operator $\Delta\mathbf{r}(t)$, we consider the case where the system has *open boundary conditions*, where the position operator $\mathbf{r}$ is naturally single-valued. In the lattice site basis, the Hamiltonian's matrix elements depend on the vector potential $\mathbf{A}$ in the following way:

$$H_{ab}(\mathbf{A}) = H_{ab}e^{i\mathbf{A}\cdot(\mathbf{r}_a-\mathbf{r}_b)}. \tag{S16}$$

Consequently, $\frac{\partial H(t)}{\partial\mathbf{A}} = i[\mathbf{r},H(t)]$, and we find $\partial_t\Delta\mathbf{r}(t) = \partial_t\mathbf{r}(t)$, where $\mathbf{r}(t) = U^\dagger(t)\mathbf{r}U(t)$ is the time-evolved position operator in the Heisenberg picture. Using the initial condition $\Delta\mathbf{r}(0)=0$, we find

$$\Delta\mathbf{r}(t) = \mathbf{r}(t) - \mathbf{r}(0). \tag{S17}$$

For a system with periodic boundary conditions (e.g., a torus), it is not possible to write $\Delta\mathbf{r}(t)$ as a difference of initial and final positions, as in the above equation. However, when $\Delta\mathbf{r}(t)$ acts on a state $|\psi\rangle$ that stays localized within a region S that is much smaller than the size of the torus, we can ignore the boundary conditions and write

$$\Delta\mathbf{r}(t)|\psi\rangle = (\mathbf{r}_S(t) - \mathbf{r}_S)|\psi\rangle, \tag{S18}$$

where $\mathbf{r}_S$ is a position operator defined with a branch cut outside S. (We note that the right-hand side does not depend on the exact location of the branch cut, as long as it is located far outside the region S.)

Relationship with magnetization density

Having defined the displacement operator, we now rewrite the winding number formula (S14) in terms of this operator. Using the definition in Eq. (S15), we replace $\tilde{U}^\dagger \partial_{\mathbf{A}} \tilde{U}$ with $i\Delta\tilde{\mathbf{r}}(t)$, where $\Delta\tilde{\mathbf{r}}(t)$ is the displacement operator for the system governed by $\tilde{H}(t)$. Similarly, as noted in the text below Eq. (S15), we may replace $\tilde{U}^\dagger(\partial_{\mathbf{A}}\tilde{H})\tilde{U}$ with $-\partial_t \Delta\tilde{\mathbf{r}}(t)$. Thus we obtain

$$W[U] = \frac{1}{2L^2}\int_0^{2T} dt\, \mathrm{Tr}\left(\Delta\tilde{\mathbf{r}}(t) \times \partial_t \Delta\tilde{\mathbf{r}}(t)\right). \tag{S19}$$

The integrand in Eq. (S19) above has a very similar form to that of the magnetization, Eq. (1) of the main text. It remains to show that this expression, which involves the displacement operator defined in Eq. (S15), precisely reduces to the magnetization discussed in the main text.

Writing out the trace in terms of the (localized) Floquet eigenstates $\{|\psi_n\rangle\}$, and using Eq. (S18), we obtain

$$W[U] = \frac{1}{2L^2}\int_0^{2T} dt \sum_n \langle\psi_n|(\tilde{\mathbf{r}}_n(t) - \mathbf{r}_n) \times \partial_t \tilde{\mathbf{r}}_n(t)|\psi_n\rangle.$$

Here $\tilde{\mathbf{r}}_n(t) \equiv \tilde{U}^\dagger(t)\mathbf{r}_n\tilde{U}(t)$, where $\mathbf{r}_n$ is a position operator, defined with a branch cut far away from the region where the state $|\psi_n\rangle$ is localized. Using that $\tilde{U}(2T) = 1$, such that $\tilde{\mathbf{r}}_n(2T) = \tilde{\mathbf{r}}_n(0) = \mathbf{r}_n$, we find

$$W[U] = \frac{1}{2L^2}\int_0^{2T} dt \sum_n \langle\psi_n|\tilde{\mathbf{r}}_n(t) \times \partial_t \tilde{\mathbf{r}}_n(t)|\psi_n\rangle. \tag{S20}$$

In the first half of the driving, i.e., for $0 \le t \le T$, the system evolves according to the original Hamiltonian $H(t)$. Here $\tilde{\mathbf{r}}_n(t) = \mathbf{r}_n(t) \equiv U^\dagger(t)\mathbf{r}_n U(t)$, where $U(t)$ is the corresponding evolution operator of the original system. In the second half of the driving, from T to $2T$, the Hamiltonian of the system is given by $\tilde{H}(t) = -H_{\mathrm{eff}}$, and the time-evolution operator is given by $\tilde{U}(t) = e^{-iH_{\mathrm{eff}}(2T-t)}$. Using $\tilde{\mathbf{r}}_n(t) = \tilde{U}^\dagger(t)\mathbf{r}_n\tilde{U}(t)$, we then have (for $T \le t \le 2T$):

$$\tilde{\mathbf{r}}_n(t) \times \partial_t \tilde{\mathbf{r}}_n(t) = -ie^{iH_{\mathrm{eff}}(2T-t)}\mathbf{r}_n \times [\mathbf{r}_n, H_{\mathrm{eff}}]e^{-iH_{\mathrm{eff}}(2T-t)}.$$

Using $H_{\mathrm{eff}} = \sum_n P_n\varepsilon_n$, where $P_n = |\psi_n\rangle\langle\psi_n|$, we obtain

$$\langle\psi_n|\tilde{\mathbf{r}}_n(t) \times \partial_t \tilde{\mathbf{r}}_n(t)|\psi_n\rangle = -i\sum_m \langle\psi_n|\mathbf{r}_n \times [\mathbf{r}_n, P_m]|\psi_n\rangle\varepsilon_m.$$

Thus the integrand in Eq. (S20) is actually constant over the interval $T \le t \le 2T$. This allows us to perform part of the integration and obtain

$$W[U] = \frac{1}{2L^2}\int_0^{T} dt \sum_n \langle\psi_n|\mathbf{r}_n(t) \times \partial_t \mathbf{r}_n(t)|\psi_n\rangle + \frac{iT}{2L^2}\sum_{m,n}\langle\psi_n|\mathbf{r}_n \times [\mathbf{r}_n, P_m]|\psi_n\rangle\varepsilon_m. \tag{S21}$$

We now argue that the last term in Eq. (S21) must be zero. To do this, we note that for a fully-localized system, the winding number is independent of the choice of the quasienergy zone (i.e., the position of the branch cut ε in $H_{\mathrm{eff},\varepsilon}$, see Ref. S1). If we shift the quasienergy cut to the gap between ε_{m_0} and ε_{m_1}, where ε_{m_0} and ε_{m_1} are the lowest- and second lowest quasienergies, respectively, the quasienergy ε_{m_0} changes by $2\pi/T$, while all other quasienergies remain the same: $\varepsilon_{m_0} \to \varepsilon_{m_0} + 2\pi/T$. The invariance of the left-hand side of Eq. (S21) under this shift of quasienergy zone implies that

$$\sum_n \langle\psi_n|\mathbf{r}_n \times [\mathbf{r}_n, P_{m_0}]|\psi_n\rangle = 0. \tag{S22}$$

Since the branch cut could be placed anywhere in the spectrum, the argument above should in fact hold for any choice of m_0. Therefore the last term in Eq. (S21) must vanish, and we arrive at

$$W[U] = \frac{1}{2L^2}\int_0^{T} dt \sum_n \langle\psi_n|\mathbf{r}_n(t) \times \partial_t \mathbf{r}_n(t)|\psi_n\rangle. \tag{S23}$$

Following the discussion in the main text, we identify

$$\frac{1}{2T}\int_0^{T} dt\, \langle\psi_n|\mathbf{r}_n(t) \times \partial_t \mathbf{r}_n(t)|\psi_n\rangle = \langle M\rangle_T^{(n)} \tag{S24}$$

as the time-averaged magnetization of Floquet eigenstate n. Hence

$$W[U] = \frac{T}{L^2}\langle M\rangle_T, \quad \langle M\rangle_T = \sum_n \langle M\rangle_T^{(n)}, \tag{S25}$$

where $\langle M\rangle_T$ is the total magnetization of the system when all states are occupied (on a torus). Using $\langle M\rangle_T = L^2\bar{m}_\infty$, we finally arrive at

$$\bar{m}_\infty = \frac{W[U]}{T}. \tag{S26}$$

This is what we set out to show: the magnetization density of a fully-localized Floquet system is a topological invariant, with its value equal to the winding number identified in Ref. S1, divided by the driving period, T.

Measurement of magnetization in a cold atoms experiment

In this section, we prove Eq. (10) in the main text. We show that the time-averaged magnetization can be measured via the net y-component of total (pseudo)-spin of a cloud of two-component cold atoms subjected to a spin-dependent artificial magnetic field. In this section, we will work in the Heisenberg picture. For an individual atom in the experiment, the wave function before the measurement is given by

$$|\psi\rangle = \frac{1}{\sqrt{2}}|\chi\rangle \otimes \left(|\uparrow\rangle + |\downarrow\rangle\right), \tag{S27}$$

where $|\chi\rangle$ denotes the orbital part of the atom's wave function, and the tensor product separates the orbital and spin parts of the wave function. The time evolution operator of the system for the case where the spin-dependent effective field acts only on the $|\uparrow\rangle$ spin component is given by

$$\mathbb{U}(\tau) = U_B(\tau) \otimes |\uparrow\rangle\langle\uparrow| + U_0(\tau) \otimes |\downarrow\rangle\langle\downarrow|, \tag{S28}$$

where $U_B(\tau)$ is the time-evolution operator (acting only on the system's orbital degrees of freedom) when a uniform field B is applied.

After an evolution time τ in the presence of the effective field B, the atom's wave function is given by

$$|\psi(\tau)\rangle = \frac{1}{\sqrt{2}} \left(U_B(\tau)|\chi\rangle \otimes |\uparrow\rangle + U_0(\tau)|\chi\rangle \otimes |\downarrow\rangle \right). \tag{S29}$$

Hence, at time τ, the expectation value of the y-spin operator $\sigma_y = \frac{i}{2}(|\uparrow\rangle\langle\downarrow| - |\downarrow\rangle\langle\uparrow|)$ is given by

$$\langle\sigma_y(\tau)\rangle = \frac{i}{2}\langle\chi| \left(U_B^\dagger(\tau)U_0(\tau) - U_0^\dagger(\tau)U_B(\tau) \right) |\chi\rangle. \tag{S30}$$

Using $U_B(\tau) = U_0(\tau) + B\frac{\partial}{\partial B}U_B(\tau)|_{B=0} + \mathcal{O}(B^2)$, valid in the linear response regime of weak fields, we obtain

$$\langle\sigma_y(\tau)\rangle = -iB\langle\chi| \left(U_0^\dagger(\tau)\frac{\partial}{\partial B}U_0(\tau) \right) |\chi\rangle + \mathcal{O}(B^2), \tag{S31}$$

where for brevity we write $\frac{\partial}{\partial B}U_B(\tau)|_{B=0} \equiv \frac{\partial}{\partial B}U_0(\tau)$. To arrive at Eq. (S31), we used the identity $\frac{\partial}{\partial B}U_0^\dagger \cdot U_0 = -U_0^\dagger \cdot \frac{\partial}{\partial B}U_0$. Using Eq. (S2) we obtain the following result, which is valid on short times where the spin precession angle remains small:

$$\langle\sigma_y(\tau)\rangle = B\int_0^\tau dt\, \langle\chi(t)|M(t)|\chi(t)\rangle + \mathcal{O}(B^2). \tag{S32}$$

Here we have introduced the operator $M(t)$ as a shorthand for $-\frac{\partial H(t)}{\partial B}$. We note that this operator, and its expectation values (for non-stationary states), in general depend on the implementation of the gauge field, see discussion below.

The above result, Eq. (S32), holds for an individual atom. For a droplet of many non-interacting atoms the droplet's total y-spin $\langle S_y\rangle$ can be obtained by summing together their individual contributions:

$$\langle S_y(NT)\rangle = BNT\sum_j \langle M\rangle_{NT}^{(j)} + \mathcal{O}(B^2), \tag{S33}$$

where the sum runs over all atoms j in the droplet, and $\langle M\rangle_\tau^{(j)}$ denotes the time-averaged expectation value of $M(t)$ for the atom j, taken over the interval $0 \le t \le \tau$. Importantly, for long times, $N \to \infty$, the particle density is stationary and $\langle M\rangle_{NT}^{(j)}$ becomes gauge independent. In this limit, $\sum_j \langle M\rangle_{NT}^{(j)} \to \langle\langle M\rangle\rangle$ and we find

$$\lim_{NT\to\infty} \frac{1}{BNT}\langle S_y(NT)\rangle = \langle\langle M\rangle\rangle + \mathcal{O}(B). \tag{S34}$$

For a finite number of periods N, there will in general be a transient correction to the relation in Eq. (S34) above. Consider a filled droplet, as described in the main text, where the many-body state is described by a single Slater determinant. Within such a state, atoms localized deep inside the bulk of the droplet (i.e., centered many localization lengths from its boundary), where all sites are filled, can be taken to be occupying Floquet eigenstates. For an atom j initialized in a Floquet eigenstate n, $\langle M\rangle_{NT}^{(j)} = -\frac{\partial\varepsilon_n}{\partial B}$ for any integer number of periods, N. Thus atoms in the bulk do not give any transient corrections to Eq. (S34). However, an atom j localized near the boundary of the droplet does not generically occupy a single Floquet eigenstate. In this case, the contribution of atom j to the total density is not stationary over a single period, and $\langle M\rangle_{NT}^{(j)}$ generally depends on N. Thus the motion of atoms localized in a strip of width $\sim \xi$ along the boundary of the droplet produces a transient deviation of $\frac{1}{BNT}\langle S_y(NT)\rangle$ from its long-time asymptotic value $\langle\langle M\rangle\rangle$.

The non-universal transient depends on details of the implementation, including in particular the choice of "gauge" used for producing the effective spin-dependent magnetic field. That is, the spin rotation of an atom moving through the lattice depends explicitly on the "vector potentials" $\mathbf{A}_\uparrow$ and $\mathbf{A}_\downarrow$ for up and down spins, respectively, and not only on the effective magnetic fields $\mathbf{B}_\uparrow = \nabla\times\mathbf{A}_\uparrow$ and $\mathbf{B}_\downarrow = \nabla\times\mathbf{A}_\downarrow$. Independent "gauge" transformations of $\mathbf{A}_\uparrow$ and $\mathbf{A}_\downarrow$ correspond to position-dependent spin rotations around the z-axis. Since the system is initialized and measured in a fixed, spatially uniform frame, there is no symmetry under spin-dependent gauge transformations.

We now estimate the magnitude of the transient correction. To do so, we consider the case of a circular droplet of radius R, where the magnetic field is implemented in the symmetric gauge (here the origin of the coordinate system is located in the droplet's center). In the symmetric gauge, recall from Sec. that $M(t) = -\frac{\partial H(t)}{\partial B} = \frac{1}{2}\hat{\mathbf{z}}\cdot(\mathbf{r}\times\dot{\mathbf{r}}(t))$. For an atom at the boundary of the droplet we write $\mathbf{r}(t) = \mathbf{R} + \delta\mathbf{r}(t)$, where $\mathbf{R} = \langle\langle\mathbf{r}(t)\rangle\rangle$ is a vector of length $\sim R$ pointing from the origin to the atom's long-time-averaged position, and $\delta\mathbf{r}(t)$ describes the motion around this point, with $|\delta\mathbf{r}| \sim \xi$. The time-averaged expectation value of M for an atom in the boundary region is then

$$\langle M\rangle_{NT}^{(j)} = \frac{-i}{2}\hat{\mathbf{z}}\cdot\left[\mathbf{R}\times\langle\delta\dot{\mathbf{r}}\rangle_{NT} + \langle\delta\mathbf{r}\times\delta\dot{\mathbf{r}}\rangle_{NT}\right]. \tag{S35}$$

The first term yields a contribution to $\langle M\rangle_{NT}$ of order $R\langle\dot{r}_\parallel\rangle_{NT}$, where $\dot{r}_\parallel(t)$ denotes the tangential com-

ponent of the atom's velocity along the boundary. Since the atom must remain confined within a region of linear dimension ξ for all times, the N-period average of the tangential velocity takes a typical value of order ξ/NT. Therefore we expect the corresponding transient contribution to $\langle M\rangle_{NT}^{(j)}$ to have a magnitude at most $\sim \frac{R\xi}{NT}$. Assuming that the atoms are initially randomly distributed within their respective localization areas (this is assured by letting particle density in the droplet reach a steady profile before the measurement begins), the *sign* of $\langle \dot{r_\parallel}\rangle_{NT}$ is expected to be random. Any transient contributions to $\langle M\rangle_{NT}^{(j)}$ from the second term in Eq. (S35) involving $\delta\mathbf{r}\times\delta\dot{\mathbf{r}}$ are expected to be relatively suppressed by a factor ξ/R, and we ignore them below.

Having estimated the scale of the transient contribution to $\langle M\rangle_{NT}^{(j)}$ for each boundary atom, we now infer the net contribution of all atoms to the net transient deviation of $\frac{1}{BNT}\langle S_y(NT)\rangle$ from the asymptotic value $\langle\langle M\rangle\rangle$. First, note that total number of atoms in the boundary region (a strip of width ξ around the perimeter of the droplet) is of order $R\xi/a^2$. Assuming a random sign for the contribution of each atom, we get a net transient correction with magnitude of order $\sqrt{\frac{R\xi}{a^2}}\cdot\frac{R\xi}{NT}$. Using $A_{\rm loc}=\xi^2$, and $A_{\rm filled}\sim R^2$, we thus obtain

$$\sum_j \langle M\rangle_{NT}^{(j)} = \langle\langle M\rangle\rangle + \frac{1}{NT}\mathcal{O}\left(\frac{A_{\rm loc}A_{\rm filled}}{a\sqrt{R\xi}}\right). \qquad \text{(S36)}$$

While this result was obtained for a field is implemented in the symmetric gauge, analogous arguments to those above can be used for other natural implementations, e.g. the Landau gauge, to show that the transient should have the same magnitude as above.

Using Eq. (S36) in Eq. (S33), we see that

$$\frac{\langle S_y(NT)\rangle}{BNT} = \langle\langle M\rangle\rangle + \frac{1}{NT}\mathcal{O}\left(\frac{A_{\rm loc}A_{\rm filled}}{a\sqrt{R\xi}}\right) + \mathcal{O}(B). \qquad \text{(S37)}$$

Hence the cloud's total magnetization can be extracted from the asymptotic behaviour of the growth rate of $\langle S_y(\tau)\rangle$ in the long-time limit. The result for the average y-spin *per particle* $\langle\overline{\sigma}_y(NT)\rangle$, in Eq.(10) in the main text, is obtained by dividing both sides of Eq. (S37) with the total number of atoms, $A_{\rm filled}/a^2$.

The "long time limit" in which the magnetization can be extracted should be understood as a time that is long compared with the damping of transients due to the system's initialization, but still short enough that the atoms' spin precession angle is small. The necessary separation of timescales can be guaranteed both by working at small fields, B, and by taking a large enough droplet (since the transient correction to $\langle\overline{\sigma}_y(NT)\rangle$ decays as $1/\sqrt{R}$). In practice, our numerics show that the transients can be made quite small for square droplets of only a few tens of lattice sites per side (see below and main text).

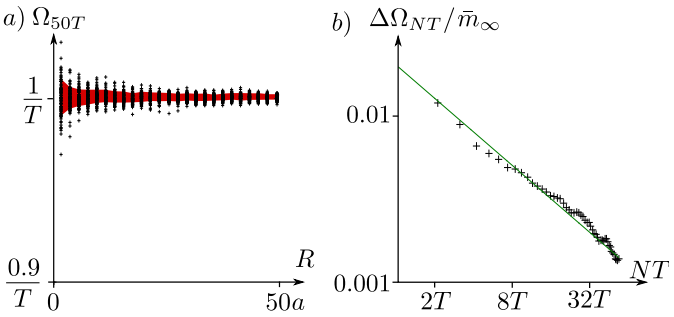

FIG. S1. Statistical behaviour of the normalized growth rate Ω_{NT}, whose saturation value yields the long-time-averaged magnetization density. a) Normalized growth rate Ω_{NT} as function of droplet size R, obtained for 100 disorder realizations, with parameters set as in the main text (for each R, each realization corresponds to one black cross). The red shading indicates the interval within one standard deviation from the data points' mean. b) Deviation $\Delta\Omega_{NT}$ of the net y-spin growth rate from the expected saturation value $\bar{m}_\infty = 1/T$, as a function of the averaging time NT, taken as an rms-average over 100 disorder realizations. The data are shown in a logarithmic plot.

Numerical simulation

Here we provide additional details from the numerical simulations, beyond what was discussed in the main text. The magnetic field in the simulation was implemented in the Landau gauge, $\mathbf{A} = (0, -B(x - x_0))$, where x_0 is located in the center of the lattice.

To explore the generic behavior of the system in the parameter regime used in the main text, we find and diagonalize the Floquet operator for 100 random disorder realizations, on a lattice of 80×80 sites with periodic boundary conditions. Among all Floquet eigenstates across these 100 realizations, we find the largest localization length to be $11.7a$, where a is the lattice constant. Thus we are well within the fully-localized, AFAI regime. We furthermore have compiled statistics to demonstrate how the normalized growth rate $\Omega_{NT}\equiv\frac{1}{Ba^2NT}\langle\overline{\sigma}_y(NT)\rangle$ converges to the quantized value with system size and averaging time, which we now discuss.

In Fig. S1a we show the time-averaged magnetization density after 50 periods as function of R (the side length of the filled squared droplet) for each of the 100 realizations. For each value of R, each black cross indicates the the value obtained for a specific realization. The red area marks the interval within one standard deviation from the mean value of Ω_{50T}, obtained from the 100 realizations. For *all* disorder realizations we see that Ω_{50T} rapidly converges to the quantized value as the size of the filled region, L, is increased.

To see how the average magnetization converges to the quantized value with the averaging time, NT, we investigate the deviation $\Delta\Omega_{NT}$ of Ω_{NT} from the quantized

value $\bar{m}_\infty = 1/T$ as a function of N. The value of $\Delta\Omega_{NT}$ is obtained as a root-mean-squared deviation, taken over the 100 realizations, in the case where a region of 50×50 sites is initially occupied. The data are shown in a log-log plot in Fig. S1b. The linear trend indicates that the deviation decreases with a power-law scaling behaviour. From a linear fit (green line), we find that the deviation from the quantized value decreases as $(NT)^{-0.64}$.

[S1] P. Titum, E. Berg, M. S. Rudner, G. Refael, and N. H. Lindner, Phys. Rev. X **6**, 021013 (2016).

[S2] M. B. Hastings and S. Michalakis, Communications in Mathematical Physics **334**, 433 (2015), ISSN 1432-0916.